J. Anat. (2007) **211**, pp26–36 doi: 10.1111/j.1469-7580.2007.00744.x

Functional respiratory morphology in the newborn quokka wallaby (*Setonix brachyurus*)

A. N. Makanya,[1] S. A. Tschanz,[2] B. Haenni[2] and P. H. Burri[2]

[1]*Department of Veterinary Anatomy & Physiology, University of Nairobi, Kenya*
[2]*Institute of Anatomy, University of Berne, Switzerland*

Abstract

A morphological and morphometric study of the lung of the newborn quokka wallaby (*Setonix brachyurus*) was undertaken to assess its morphofunctional status at birth. Additionally, skin structure and morphometry were investigated to assess the possibility of cutaneous gas exchange. The lung was at canalicular stage and comprised a few conducting airways and a parenchyma of thick-walled tubules lined by stretches of cuboidal pneumocytes alternating with squamous epithelium, with occasional portions of thin blood–gas barrier. The tubules were separated by abundant intertubular mesenchyme, aggregations of developing capillaries and mesenchymal cells. Conversion of the cuboidal pneumocytes to type I cells occurred through cell broadening and lamellar body extrusion. Superfluous cuboidal cells were lost through apoptosis and subsequent clearance by alveolar macrophages. The establishment of the thin blood–gas barrier was established through apposition of the incipient capillaries to the formative thin squamous epithelium. The absolute volume of the lung was 0.02 ± 0.001 cm^3 with an air space surface area of 4.85 ± 0.43 cm^2. Differentiated type I pneumocytes covered 78% of the tubular surface, the rest 22% going to long stretches of type II cells, their precursors or low cuboidal transitory cells with sparse lamellar bodies. The body weight-related diffusion capacity was 2.52 ± 0.56 mL O_2 min^{-1} kg^{-1}. The epidermis was poorly developed, and measured 29.97 ± 4.88 μm in thickness, 13% of which was taken by a thin layer of stratum corneum, measuring 4.87 ± 0.98 μm thick. Superficial capillaries were closely associated with the epidermis, showing the possibility that the skin also participated in some gaseous exchange. Qualitatively, the neonate quokka lung had the basic constituents for gas exchange but was quantitatively inadequate, implying the significance of percutaneous gas exchange.

Key words development; lung; marsupial; morphology; morphometry; neonate; quokka; ultrastructure.

Introduction

The neonates of metatheria are known to be extremely atricial at the time of birth, further development taking place in the maternal pouch. Obviously in eutherian mammals the lung needs to be adequately developed before birth to ensure sufficient gas exchange and hence survival in the neonate. The quokka wallaby, which is the subject of the current study, differs from those other species in that the canalicular stage of lung development is encountered postnatally, the entire process of postnatal lung development taking up to 180 days (Makanya et al. 2001). Although the quokka lung has been postulated to be at canalicular stage at birth, the youngest animal reported this far was 3 days old and hence the morphological and functional status of the lung in the first day of life remains obscure. The unique finding in the neonate quokka lung opens a new window to a better understanding of lung development given that in all the other animals reported this far, the canalicular stage is confined to the prenatal period (e.g. Burri, 1999), making it logistically difficult to access the lung for manipulative studies. Furthermore, the prenatal lung is fluid-filled and not ventilated, thus making comparisons with premature neonates much more complicated.

In eutherian mammals presentation of the canalicular stage postnatally would be grossly premature and most likely fatal. In most animals at birth the lung has reached a level where it is capable of gas exchange; otherwise, an alternative organ system has to be temporarily recruited (e.g. Mortola et al. 1999; Frappell & Mortola, 2000) or artificial intervention employed to sustain life. The attainment of functional capacity in the lung entails not only the development of an adequate surfactant system, but also conversion of the cuboidal epithelium of the pseudoglandular

Correspondence
Dr A. N. Makanya, Department of Veterinary Anatomy & Physiology, University of Nairobi, PO Box 30197-00100, Nairobi, Kenya. T: +254 20 4446764; F: +254 20 4451770; E: makanya@uonbi.ac.ke

Accepted for publication *16 March 2007*

stage to a squamous epithelium and subsequent apposition of the latter to blood capillaries to form thin blood–gas barriers. The attenuation of type I pneumocytes (Mercurio & Rhodin, 1976) and progressive approximation of the parenchymal capillaries to the epithelial layer occurs by a reduction in the interstitial tissue (Burri & Weibel, 1977).

In the recent past it has been demonstrated that the skin is an important component of the gas exchange system in the neonate marsupial. In the tiny neonate Julia Creek dunnart (*Sminthopsis douglasi*) the skin contributes almost the total gaseous metabolism at birth declining to a third by the third postnatal week (Frappell & Mortola, 2000), which prompts the question of whether the marsupial lung is adequately developed to handle gaseous requirements of the neonate at birth (MacFarlane & Frappell, 2001). In the neonate tammar wallaby (*Macropus eugenii*) the skin contributes about 30% of all gas exchange at birth declining to 14% by day 6 (MacFarlane et al. 2002). In the current study, we have studied the qualitative and quantitative characteristics of the parenchymal components of the lung of the neonate quokka, with the finding that, quantitatively, lung morphology may limit gas exchange at birth.

Materials and methods

Experimental animals

Three neonate quokka joeys were obtained from the Animal Station in Shenton Park, University of Western Australia, Perth, as detailed previously (Makanya et al. 2001). Pouches of selected quokka dams were examined and if a quokka joey was present, this was removed and the dams earmarked. Pouches were subsequently examined from the 24th day after joey-extraction to obtain a newborn joey at the earliest possible time.

Anaesthesia, fixation and tissue sampling

Quokka joeys were anaesthetized with an intraperitoneal mixture of Vetranquil®, Xylapan® and Narketan® given at dosage rates of 0.1, 1 and 10 mg per 100 g body weight, respectively. The joeys were fixed by total immersion in a solution of 2.5% glutaraldehyde in 0.1 M cacodylate buffer (pH 7.4, 350 mOsm) as detailed previously, then severing the neck to allow intratracheal infiltration of the fixative. Lungs were removed under a dissecting microscope. It was ensured that the lungs were well expanded. This was achieved by ascertaining that the lobes were closely applied to the walls of the pleural cavity. Volumes of the right lung lobe together with the accessory lobe and that of the left lung lobe were estimated by fluid displacement (Scherle, 1970). The entire left lung lobe was processed for light microscopic (LM) morphometry while the right lung and accessory lobes were diced and processed for transmission electron microscopy (TEM) and scanning electron microscopy (SEM).

Lung morphology and morphometry

For LM, selected tissue blocks obtained from the left lung were dehydrated in ascending concentrations of ethanol and embedded in paraffin wax. Serial sections were obtained at a nominal thickness of 4 μm using a Reichert Jung microtome, stained with haematoxylin and eosin and viewed on an Olympus Vanox S light microscope. For ultrastructural studies tissue blocks were postfixed in osmium tetroxide, block stained using uranyl acetate, dehydrated through ascending concentrations of ethanol and embedded in epoxy resin. Ultrathin sections were obtained at 90 nm, counterstained with lead citrate and viewed on a Philips EM-200 microscope or Philips EM-300 microscope. For SEM, tissue samples were obtained from the right lung and dehydrated in ascending concentrations of ethanol, critical-point dried in liquid carbon dioxide and subsequently sputter-coated with gold. The specimens were mounted on brass stubs and viewed on a Philips XL30 FEG scanning electron microscope. Tissue sampling both at light and electron microscopy were done as detailed previously (Burri et al. 2003; Makanya et al. 2003). Five blocks per animal obtained from the left lung lobe and five from the right lung were processed for LM and EM morphometry, respectively.

LM morphometry

At LM morphometry the volume densities of the lung parenchyma (Vvp) and non-parenchyma (Vvnp) were obtained by point counting methods. The parenchyma was taken to comprise the tubular lumina (Va) (no saccules or alveolar spaces at this age) and the tissue surrounding the lumina (Vs), except for the large blood vessels (≥ 25 μm in diameter) and the conducting airways. The non-parenchyma was taken to include the large blood vessels and the very few primitive airways. The proportions of the connective tissue surrounding the large blood vessels and the conducting airways were negligibly small. The absolute non-parenchymal parameters estimated included the volume of the conducting airways, the volume of coarse blood vessels, and the volume of non-parenchymal connective tissue. Sections were analysed with an Olympus BHS light microscope equipped with a moving stage and a projection screen designed for morphometry. On the viewing screen the final magnification was ×312. The screen contained a single static point and the section was moved in such a way that the point sampled the entire tissue field by field. All points on parenchyma and those on non-parenchyma and its respective components were scored using the STEPone computer program (Humbert et al. 1990). From points obtained, volume densities were estimated as fractions of the containing volume.

The volume of the parenchyma Vvp, for example, was calculated from the equations:

$$Vvp = Pp/Ptot \quad \text{and} \quad Vp = Vvp \times VL$$

where VL is the volume of the lung, and Pp and Ptot are point counts on parenchyma and total number of points on the reference space, respectively. Differential counts of points on the constituent components of both the parenchyma (i.e. air spaces and septal tissue) and the non-parenchyma (blood vessels, airways, connective tissue) were also done to obtain their respective volume densities and subsequently their absolute volumes.

TEM morphometry

Five blocks of tissue per animal were used for TEM morphometry. Ultrathin sections were prepared and photographs of the quadrants with parenchymatous tissue were taken in a consecutive manner, starting at a random position on the top left hand corner of the grid, while scoring all the quadrants covered by the air spaces. Whenever non-parenchymatous tissue was within the quadrant no photograph was taken. Eight photographs per section were obtained on a 35-mm film and contact positive copies of the film prepared. The films were viewed on a projection screen mounted on a morphometry board at a final magnification of ×12 000. Volume and surface densities of the various targeted components as well as the arithmetic and harmonic mean thicknesses were obtained using the STEPone morphometry program (Humbert et al. 1990). To score point and intersection counts, a transparent M168 test grid (Weibel, 1979) was used and the data fed directly into the STEPone program for calculation of totals. Microsoft Excel was then used to compute the various parameters. The harmonic mean thickness of the blood–gas barrier τhb was estimated as a single entity using the method proposed by Weibel et al. (1993). The Intercepts Program (Humbert et al. 1990) was used to calculate τhb.

The arithmetic mean barrier thickness τt was estimated from the formula

$$\tau t = -\frac{Vst}{(Sa + sc)/2}$$

where Vst is the volume of tissue of the septum, including the epithelial volume (VepI, VepII), the interstitial tissue volume (Vi) and the endothelial volume (Ven). Sa and Sc are the airspace and capillary surface areas, respectively. A detailed account of the sampling procedure has been given previously (Burri et al. 2003).

Estimation of volumes

The proportions of the various components of the parenchyma, i.e. airspaces (Vva), capillary lumina (Vvc), erythrocytes (Vve), endothelium (Vven), type I pneumocytes (VvepI), type II pneumocytes (VvepII), interstitial tissue (Vvi), and of the total septal volume (Vs) were obtained from point counts. To obtain the absolute values for volumes (V), the various proportions were multiplied with the reference volume and the proportion of lung parenchyma:

$$Vx = Vvx \times Vvp \times VL$$

where Vx is the volume of the component being estimated and Vvx is its volume density.

Estimation of surface areas

These were obtained by intersection counting on EM sections. The surface density of any surface is denoted as Sv and is given by the formula:

$$Sv = 2Ix/Ltot,$$

where Ix is the number of intersection counts between the test lines and the surface of interest and Ltot is the total length of test lines on the reference volume (i.e. on the parenchymal tissue).

Intersection counts with the epithelial surface were used to obtain the surface densities of airspaces (Sva), and intersection counts with the endothelial surface were used to obtain the surface density of capillaries (Svc).

Differential estimation of the areas with differentiated thin squamous epithelium (SaI), and surface on type II cells (SaII) were estimated by scoring the intersections on the respective components. From these proportions the respective absolute values were computed. Subsequently, the surface area was estimated as

$$Sx = Svx \times Vvp \times VL$$

Estimation of the haematocrit, Hct

Haematocrit (Hct) was estimated as the ratio of the erythrocyte volume (Ve) to the volume of capillary blood (Vc). Thus, Hct = Ve/Vc.

Estimation of pulmonary diffusing capacity

The pulmonary diffusing capacity, DLO_2, was estimated using the diffusing capacities of the tissue barrier (epithelium, interstitium and endothelium) and the erythrocytes, as outlined in Weibel et al. (1993).

Thus:

$$1/DLO_2 = 1/DbO_2 + 1/DeO_2,$$

where the diffusing capacity of the barrier is

$DbO_2 = kb \times Sa/\tau hb$,

and the diffusing capacity of the erythrocytes is

$DeO_2 = \theta O_2 \times Vc$.

The diffusion constant for the combined barrier (kb) was taken to be 3.3×10^{-8} cm^2 in^{-1} mmHg^{-1}, as exemplified in Weibel et al. (1993) and θO_2, the rate of oxygen uptake by the whole blood, was calculated as $\theta O_2 = Hct \times ke$, where ke is the diffusion constant for erythrocytes (taken to be 7.158 mL O_2 min^{-1} mmHg^{-1}).

Skin morphometry

Up to five strips of body skin were obtained from arbitrary positions of the body trunk of each joey, fixed by total immersion in a solution of 2.5% glutaraldehyde and processed for TEM as detailed above. The skin strips were flat-embedded so that semithin sections perpendicular to the external surface of the skin were obtained. Assessment of epidermal thickness, thickness of the keratinized layer and the distances between the external surface and most superficial capillaries were performed by multiple measurements with a digital ruler and taking the average. The images were captured on a Leica DMRBE microscope equipped with a JVC KY-70 digital camera and connected to a computer. Measurements were made directly on the computer screen using the analySIS® software (Version 3.2, Soft Imaging System, GmbH, Münster, Germany).

Abbreviations

DbO_2, diffusion capacity of the tissue barrier; DeO_2, diffusion capacity of the erythrocytes; DLO_2, total anatomical diffusion capacity of the lung; Hct, total haematocrit; kbO_2, diffusion constant for the combined barrier; LM, light microscopy; Sa, surface area of the tubular epithelium; Sc, inner surface area of the capillary endothelia; SEM, scanning electron microscopy; TEM, transmission electron microscopy; Va, volume of the parenchymal air spaces; Vc, volume of the capillary blood; Ve, volume of the erythrocytes; Vi, volume of the interstitial tissue; VL, volume of the whole lung; Vs, volume of the septa; Vst, volume of the solid tissue of the septa; τ_{hb}, harmonic mean thickness of the tissue barrier; Θ_{O2}, rate of uptake of oxygen by whole blood; τ_t, arithmetic mean thickness of the tissue barrier.

Results

Lung structure

During the canalicular stage in the newborn joey large primitive airways, which opened into few moderately sized tubules separated by thick tissue septa (Fig. 1a,b), were present. Growing capillaries, which normally characterize this stage, were rather discrete. The walls of the airways were lined by both low cuboidal and low columnar epithelium. The lining of the airspace surface was partitioned between alternating stretches of squamous type I pneumocytes and those of the cuboidal cells. In a few isolated areas capillaries with nucleated erythrocytes appeared to abut the epithelium forming the first thin portions of gas exchange barrier with a much thinner squamous type of epithelium (Fig. 1c,d). The core tissue of the septal interstitium was predominantly mesenchymal with no definitively identifiable cell morphophenotype. A few large blood vessels were identifiable in the interstitial tissue (Fig. 1d).

Besides the type I pneumocytes and the type II cuboidal cells, the epithelia of the airspaces comprised various cell types in transitional stages (Fig. 2). Some cuboidal cells had few lamellar bodies but without microvilli, perhaps showing inclination to become type I cells. Conversion of the cuboidal type II cells to squamous type I cells involved not only the elongation and attenuation of the cells but also extrusion of the lamellar bodies (Fig. 2c). In some cases, mature portions of the blood gas barrier comprising only a thin squamous epithelium, a common basement membrane and an endothelium were encountered (Fig. 2d). Reduction of the cuboidal type II cells may be augmented also by their death and subsequent removal by alveolar macrophages as seen in some regions (Fig. 3a). Such cells were replaced by the squamous pneumocytes, which were concomitantly apposed to interstitial capillaries forming portions of thin blood–gas barrier.

In some areas, intertubular septa were lined with well-developed squamous pneumocytes but lacked the capillaries and hence no blood–gas barrier portions were formed (Fig. 3b). The interstitium in such cases was rich with mesenchymal cells and dark staining cells, which were probably precursors of blood capillaries. Indeed in such septa thin capillaries completely filled with individual cells, depicting a typical capillary sprout (Fig. 3c) were encountered. The mesenchymal tissue within the septa comprised irregularly shaped mesenchymal cells with filopodia embedded in depauperate matrix (Fig. 3b).

Lung morphometry

The morphometric details on the neonate quokka lung are provided in Tables 1 and 2. The joeys had an average body weight of 0.373 ± 0.034 g and lung volume was a meagre 0.02 ± 0.001 cm^3 partitioned between a parenchyma (92.5%) and a non-parenchyma (7.5%). Within the parenchyma, airspaces comprised the highest proportion (70.4%), followed by the interstitium (15.3%), the capillary lumen (7.5%) the epithelia (4.2%) and endothelia (2.7%). At this stage the volume of the squamous pneumocytes was similar to that of the cuboidal pneumocytes. In the non-parenchyma, airways took the greater percentage of the 7.5% (65%) while

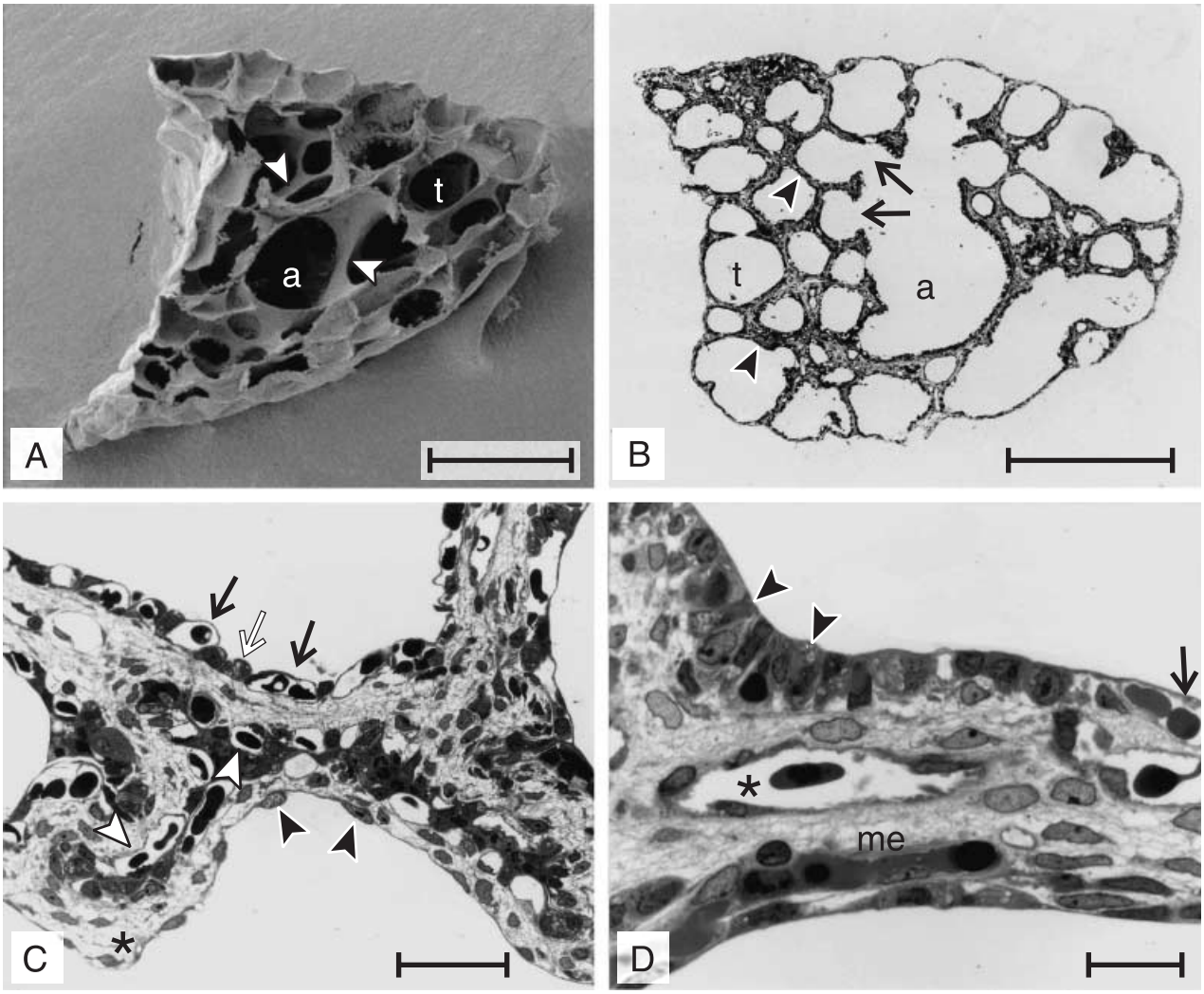

Fig. 1 Scanning (A) and light micrographs (B–D) of the lung of a quokka joey at birth showing the morphology of the parenchyma. (A) Transverse section across the entire lobe showing a large central airway (a), tubules (t) and the thick septa delineating the tubules (arrowheads). Scale bars = 500 μm. (B) A Paraffin section of an entire lobe showing a central airway (a) and tubules (t). Some tubules (arrows) open directly into the primitive airways. Note the variable thickness of the intertubular septa (arrowheads) as well as the sizes of the tubular lumina. Scale bar = 500 μm. (C) Higher magnification of the intertubular septum showing the abundant interstitial mesenchyme with undifferentiated cells (asterisk), superficial portions of thin blood–gas barrier (black arrows), cuboidal epithelium (white arrow) and some wide portions with squamous epithelium but no capillaries (black arrowheads). Within the interstitium there are many deeply situated capillaries (white arrowheads). Scale bar = 50 μm. (D) The tubular surfaces were covered by alternating stretches of cuboidal epithelium (arrowheads) and squamous epithelium (arrow). Centrally located large capillaries (asterisk) were evident and mesenchymal tissue (me) was preponderant. Scale bar = 20 μm.

the blood vessels took 30% and the connective tissue just 5% (data not shown for the latter two). The epithelial lining of the parenchymal airspaces was partitioned between the type I pneumocytes (78%) and the cuboidal cells (22%) of the cell surface. The gas exchange surface area was 4.85 ± 0.43 cm^2 and the (body mass-normalized) pulmonary diffusing capacity was 2.52 ± 0.57 mL O_2 min^{-1} $mmHg^{-1}$ kg^{-1}.

The various pulmonary morphometric parameters of the neonate quokka are compared with those of the neonate tammar wallaby and the neonatal rat in Table 2. The specific lung volume of the neonate quokka was 55.6 ± 7.0 cm^3 kg^{-1} and this was notably lower than either that of the tammar wallaby or the rat. The interairspace septa were thick, as depicted by the estimate of the septal thickness (2 × Vs/Sa) of 22.8 ± 2.0 μm compared with the newborn rat (9.3 μm). Furthermore, the capillary loading, which is the ratio of capillary volume to the surface area of airspaces (Vc/Sa), was 0.29 ± 0.01 μL cm^{-2}, a value that was higher than that of the tammar wallaby and of the newborn rat.

Skin structure and morphometry

Structural details of the skin are given in Fig. 4, and morphometric measurements are presented in Table 1. The

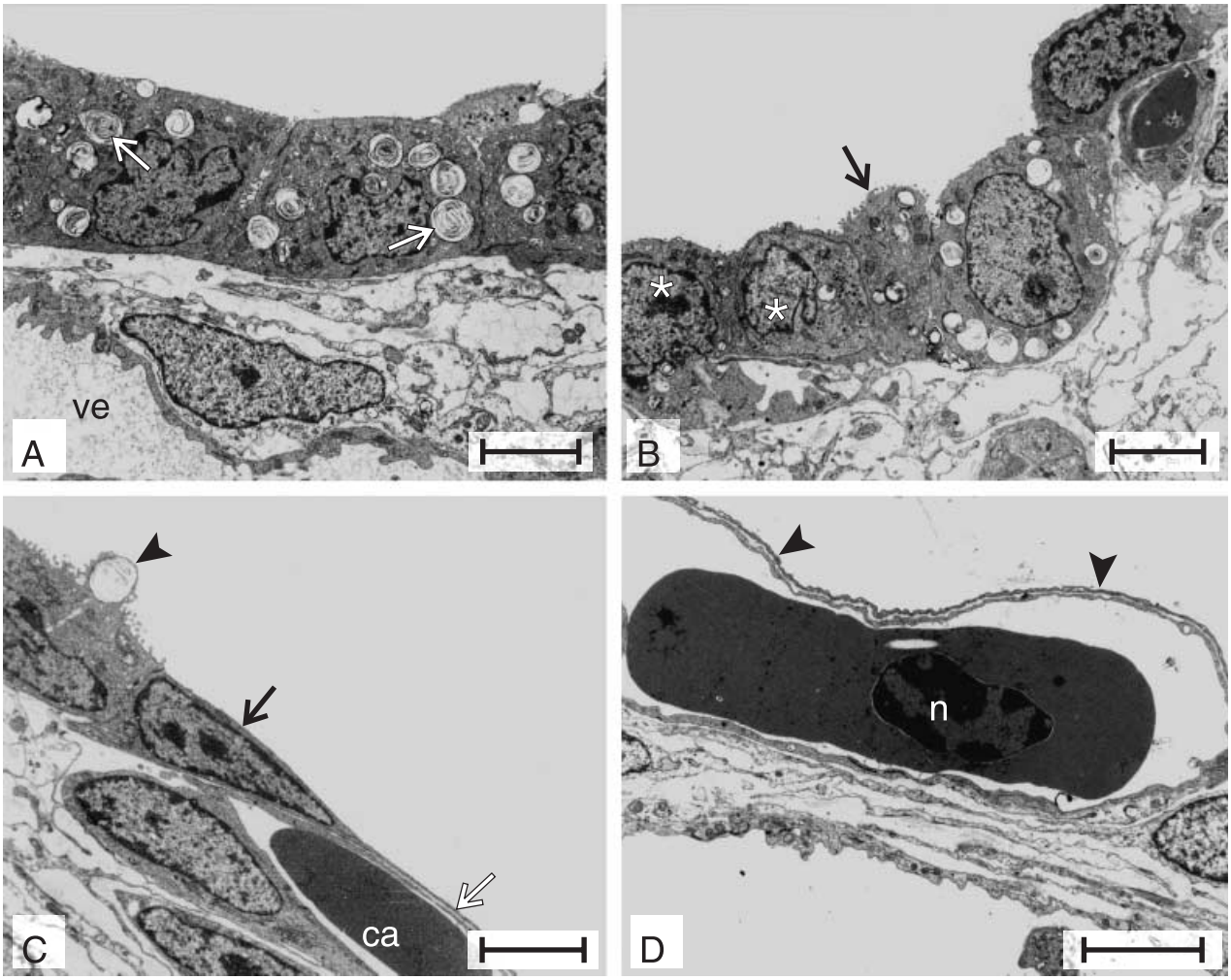

Fig. 2 Transmission electron micrographs showing the morphological changes that characterize the tubular epithelium of the neonate quokka lung with type I and type II cells and cuboidal cells in various transitional stages. (A) Micrograph showing a well-formed cuboidal epithelium endowed with lamellar bodies (white arrows). These cells notably lack microvilli and may be described as pneumoblasts with a potential to form either of the two definitive epithelial pneumocytes. Note the large blood vessel (ve) below the epithelium. Scale bar = 5 μm. (B) Some cuboidal cells may have scanty lamellar bodies while also lacking microvilli, probably showing a tendency to form type I cells (white asterisks) while others have already acquired microvilli and have abundant lamellar bodies (arrow). Scale bar = 5 μm. (C) Type II cells converting to type I pneumocytes appear to do so by extruding entire lamellar bodies (arrowhead) and flattening out (arrow). Newly formed type I pneumocytes (white arrow) may become associated with superficial capillaries (ca), thus constituting a blood–gas barrier. Scale bar = 5 μm. (D) Even at this early stage, 'mature' thin blood–gas barriers (arrowheads) with virtually no interstitial tissue were present and these comprised a thin epithelial layer, a common basement membrane and an endothelium. Most of the erythrocytes (erythroblasts) had a central nucleus (n). Scale bar = 5 μm.

skin was poorly developed and the epidermis lacked the stratification characteristic of the mammalian integument. Hairs and hair follicles were conspicuously absent and the epidermis was only discernible into a thin stratum corneum comprising up to five layers of flattened keratinocytes and a stratum basale with amorphous, elongated and rounded cells. The entire epidermis measured 29.97 ± 4.88 μm in thickness, while the stratum corneum was only 4.87 ± 0.981 μm thick. Several superficial subcutaneous capillaries were encountered, some closely apposed to the epidermis (Fig. 4). The skin diffusion barriers ranged between 30 and 35 μm thick, showing the possibility that the skin also participated in gaseous exchange.

Discussion

Lung morphology

Generally in marsupials, the lung has been reported to be in the terminal sac stage of development at birth (e.g. Runciman et al. 1996), with the exception of the quokka, which at 3 days of age was found to be at the canalicular stage (Makanya et al. 2001). The parenchymal phenotypes during pre- and postnatal lung development have been well documented (Burri, 1999; Schittny & Burri, 2003). The presence of stretches of cuboidal epithelium, a few portions of thin blood–gas barrier and tubules separated by

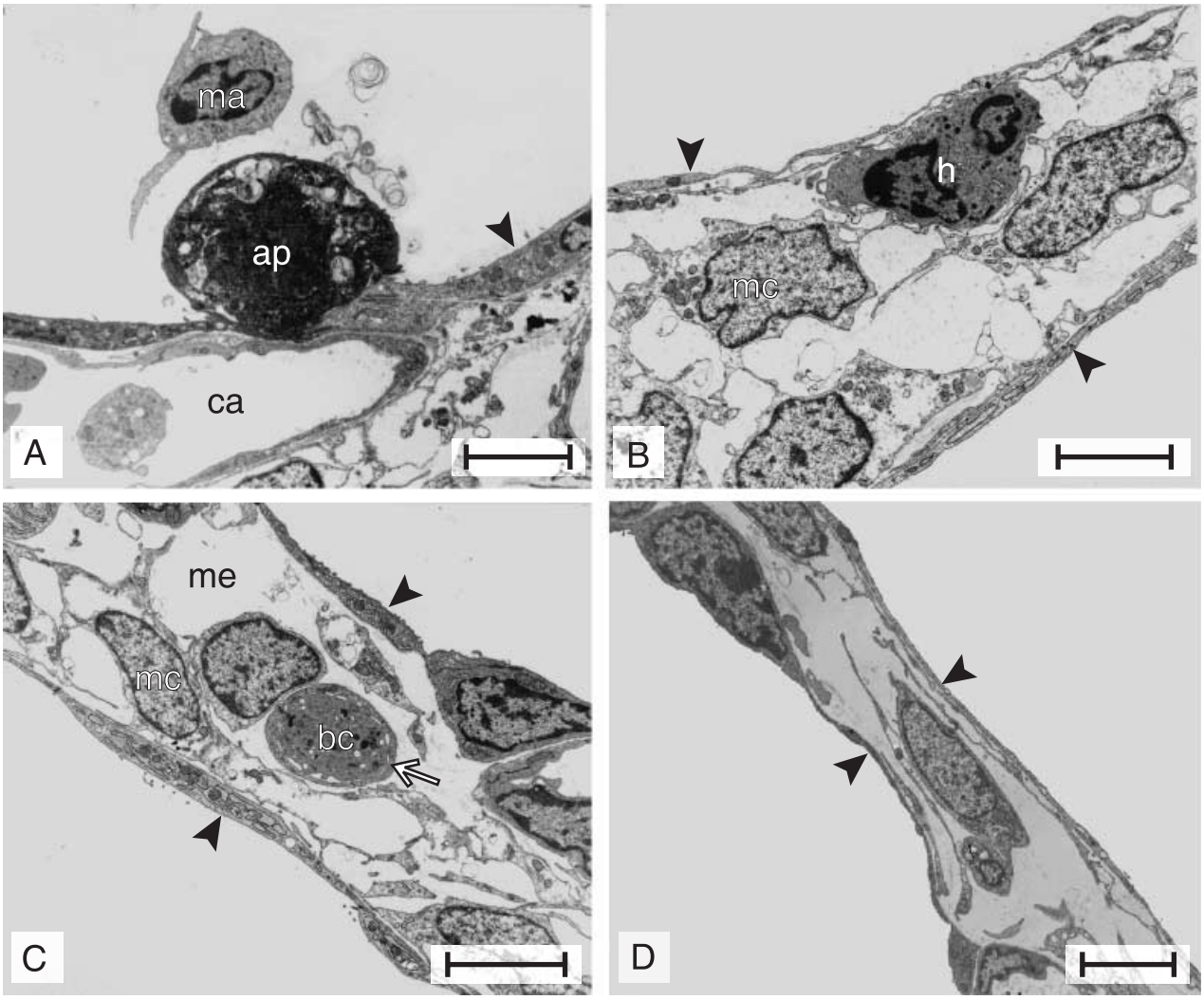

Fig. 3 Transmission electron micrographs showing various phenotypes of the intertubular septa in the lung of the neonate quokka joey. All scale bars = 5 μm. (A) The lung of the neonate quokka has the fundamental morphological characteristics necessary for gas exchange. The presence of an alveolar macrophage (ma) next to a putatively apoptotic type II cell (ap) evinces this fact. The dying type II cells are cleared by pulmonary macrophages. Such cells are replaced by newly formed type I pneumocytes (arrowhead), which approximate the sepal capillaries (ca) to form thin blood–gas barrier portions. (B) Some of the intertubular septa are covered entirely by thin type I cells (arrowheads) but lacked capillaries and hence had no blood–gas barriers. Such septa had an abundance of mesenchymal cells (mc) and also contained dark staining cells (h), which were thought to be hemangioblasts. (C) In some cases, there occurred capillary sprouts (white arrow), represented by a narrow lumen completely filled by an intraluminal blood cell (bc). Note the thin squamous epithelium (arrowheads), the loose mesenchyme (me) and uncommitted mesenchymal cells (mc). (D) Some portions of the intertubular septa were quite thin, had well-formed squamous pneumocytes (arrowheads) but lacked capillaries and hence no blood–gas barriers.

abundant interstitium with several capillaries as observed in the current study are some of the quintessential characteristics of the canalicular stage. Previous descriptions of the canalicular stage were based on specimens that were not exposed to air. The finding here that the squamous pneumocytes occupied 78% of the airspace surface points to the fact that the squamous epithelium differentiates earlier than the capillary endothelial system, and forms the superficial layer of the tripartite blood–gas barrier. The delay in the formation of capillaries and their apposition to the tubular epithelium underpins the fact that in several regions of the parenchyma the diffusion distance was quite high.

Mechanisms governing formation of the thin barrier are poorly understood (Schittny & Burri, 2003). It has been shown, however, that extrusion of lamellar bodies and stretching of the type II cells (Makanya et al. 2001) contributes to formation of the squamous pneumocytes, a fact evinced in the current study. Reduction of the type II cells involves their conversion to type I pneumocytes (Kauffman et al. 1974; Mercurio & Rhodin, 1976, 1978) as well as their loss through apoptosis (Schittny et al. 1998; Stiles et al. 2001) down to a level where they just cover 2–5% of the parenchymal airspace in adult mammals (Crapo et al. 1983). Recently, we have described novel methods of cell

Table 1 Pulmonary and cutaneous morphometric data for the three neonate quokkas. All values are means ± SEM

Parameter	Density Vvx	Absolute value Vx	Specific value Vx/BW
Lung parenchyma, p	0.926 ± 0.007	0.018 ± 0.001 cm^3	50.5 ± 6.1 $cm^3\ kg^{-1}$
Parenchymal air spaces, a	0.704 ± 0.011	0.013 ± 0.001 cm^3	35.7 ± 4.8 $cm^3\ kg^{-1}$
Parenchymal septa, s	0.296 ± 0.011	0.005 ± 0.001 cm^3	14.8 ± 1.3 $cm^3\ kg^{-1}$
Epithelia type 1, ep1	0.019 ± 0.0004	0.0004 ± 0.0001 cm^3	0.96 ± 0.13 $cm^3\ kg^{-1}$
Epithelia type 2, ep2	0.023 ± 0.0032	0.0004 ± 0.0001 cm^3	1.13 ± 0.19 $cm^3\ kg^{-1}$
Capillary lumen, c	0.075 ± 0.0023	0.0014 ± 0.0001 cm^3	3.78 ± 0.45 $cm^3\ kg^{-1}$
Capillary endothelium, en	0.027 ± 0.003	0.0005 ± 0.0001	1.39 ± 0.32 $cm^3\ kg^{-1}$
Parenchymal interstitium, i	0.153 ± 0.016	0.003 ± 0.0003 cm^3	7.57 ± 0.66 $cm^3\ kg^{-1}$
Airspace surface area, Sa	261.60 ± 11.80 cm^{-1}	4.85 ± 0.43 cm^2	1.335 ± 0.216 $m^2\ kg^{-1}$
Surface on type I cells, Sep1	78%	3.76 ± 0.36 cm^2	1.029 ± 0.159 $m^2\ kg^{-1}$
Surface on type II cells, Sep2	22%	1.05 ± 0.30 cm^2	0.291 ± 0.063 $m^2\ kg^{-1}$
Capillary surface area, Sc	302.7 ± 14.7 cm^{-1}	5.61 ± 0.41 cm^2	1.538 ± 0.225 $m^2\ kg^{-1}$
Total pulmonary diffusion capacity, DLO_2	N/A	0.00092 ± 0.00016 ml $O_2\ s^{-1}\ mmHg^{-1}$	2.52 ± 0.57 ml $O_2\ s^{-1}\ mmHg^{-1}\ kg^{-1}$
Epidermal thickness	N/A	29.97 ± 4.88 μm	N/A
Stratum corneum thickness	N/A	4.87 ± 0.98 μm	N/A

Table 2 A comparison of various pulmonary morphometric values for the neonate quokka wallaby with those of the newborn tammar wallaby and the newborn laboratory rat. Values are means ± SEM

Parameter	Quokka wallaby* *Setonix brachyurus*	Tammar wallaby† *Macropus eugenii*	Laboratory rat‡ *Rattus norvegicus*
Mass, g	0.37 ± 0.03	0.44 ± 0.04	7.2 ± 0.1
VL, cm^3	0.020 ± 0.001	0.04 ± 0.04	0.57 ± 0.01
VL, $cm^3\ kg^{-1}$	55.6 ± 7.0	74.7 ± 9.9	78.9 ± 3.2
Hct	0.49 ± 0.07	0.55 ± 0.06	N/A
τt, μm	9.21 ± 2.31	N/A	3.45 ± 0.05
τhb, μm	1.30 ± 0.31	1.4 ± 0.2	0.64 ± 0.05[b]
Sa, $m^2\ kg^{-1}$	1.34 ± 0.22	1.22 ± 0.24	5.31 ± 0.29
Sc, $m^2\ kg^{-1}$	1.54 ± 0.22	1.50 ± 0.19	5.92 ± 0.50
Vc/Sa, $\mu L\ cm^{-2}$	0.29 ± 0.1	0.22[a]	0.1[a]
2Vs/Sa, μm	22.8 ± 2.0	21.4[a]	9.2[a]
DLO_2/BW, mL $O_2\ s^{-1}\ mmHg^{-1}\ kg^{-1}$	2.52 ± 0.57	N/A	10.69[a]

Sources of data: *this study; †Runciman et al. (1996, 1998, 1999); ‡Burri et al. (1974).
[a]Data computed from mean values available in the cited studies. [b]Rat value comprising tissue barrier only.

attenuation that involve cell cutting (secarecytosis) and cell pinching-off (peremerecytosis) that result in a remarkably thin blood–gas barrier in the avian lung (Makanya et al. 2006). Whether similar mechanisms play any role in the mammalian lung is at the moment obscure. In marsupials, establishment of a functional lung prenatally takes a very short time. In the bandicoot (*Isoodon macrourus*), for example, formation of a functional lung occurs in the last 3–4 days of gestation (Gemmell & Little, 1982) while in the tammar wallaby the canalicular stage is converted into the saccular stage in the last 3 days of gestation (Runciman et al. 1996).

Lung morphometry

Many aspects of the neonate quokka strongly point to a functional inadequacy in the lung in as far as gas exchange is concerned. Besides being at canalicular stage, the specific lung volume is much lower than that of the tammar wallaby, which itself has been shown to be dependent on a percutaneous route for 33% of its oxygen requirements in the first day of life (MacFarlane et al. 2002). Furthermore, in many regions of the parenchyma the airspace surface is rather distant from the blood as capillaries are embedded deep in the thicker intertubular septa (see higher value of 2 × Vs/Sa for the wallabies compared with the rat, Table 2). In several regions a capillary trilayer with a single layer in the middle of the septum (see Fig. 1), the so-called central capillaries (Runciman et al. 1996), was encountered. Although the capillary surface area is higher than the airspace surface area, which clearly indicates well-established angiogenesis, the low diffusion capability resulting from the high diffusion distance may be part of the functional inadequacy. Furthermore, several stretches of intertubular septa without

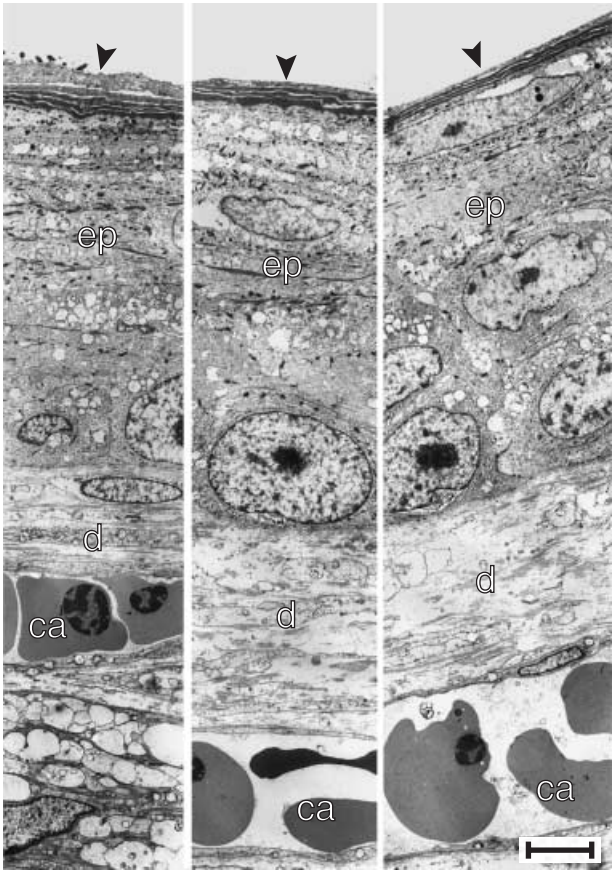

Fig. 4 Transmission electron micrographs showing the skin covering the body surface in the neonate quokka. The epidermis (ep) measured about 30 μm in thickness and there were capillaries (c) at various levels of the dermis (d), some closely associated with the epidermis. The cells of the epidermis varied in size and shape, from rounded to elongate and narrow or even squamous towards the surface. A thin layer of keratin formed the outer covering of the skin (arrowheads), but hairs were absent. Scale bar = 5 μm.

capillaries were encountered. Compared with older joeys, the estimate of the diffusing capacity in the neonate quokka is remarkably lower, reaching, for example, only half the specific value of 5-day-old joeys, which is estimated at 4.77 mL O_2 s^{-1} $mmHg^{-1}$ kg^{-1} (Burri et al. 2003).

The canalicular stage is characterized by massive formation of blood vessels within the interstitium by angiogenesis, which entails formation of new vessels from existing ones (Hall et al. 2002) as well as vasculogenesis, which is the *de novo* formation of vessels from precursor cells (deMello & Reid, 2000). Apposition of the capillaries to the attenuating epithelium results in a thin blood–gas barrier. The high capillary loading seen in the neonate quokka is indicative of the angiogenic phase of the canalicular stage, but many such capillaries are deeply located in the septa and are as such not adequately exposed to air (Runciman et al. 1996). Additionally, it has to be kept in mind that the airspace surface area is very small in these animals at birth. Generally, it appears that Sc exceeds Sa in the mammalian neonate (Tables 1 and 2), whereas, in adults, Sa slightly exceeds Sc (Burri et al. 2003). Although the quokka lung shows qualitative characteristics of a gas-exchanging organ, quantitatively, this organ is not well developed to meet the metabolic demands at birth. Furthermore, efficient gas exchange may be confounded by poor architecture of the extant structures and by functional prematurity in organs related to pulmonary ventilation such as the muscles (MacFarlane & Frappell, 2001; Frappell & MacFarlane, 2006).

Gas exchange through the skin

Percutaneous gas exchange is known to be the primary mode of gas exchange in lungless salamanders of the family Plethodontidae. The lungless European salamander (*Salamandra maculosa*) has an epidermis measuring 40–60 μm in thickness with a 5-μm-thick stratum corneum containing 8–12 layers of keratinocytes (Spearman, 1968). The only surfaces available for the exchange of respiratory gases in this animal are the skin and the inside surfaces of the mouth and pharynx (Whitford & Hutchison, 1965). Cutaneous gas exchange in adult mammals is limited by the poor gas diffusion properties of the skin tissues (MacFarlane et al. 2002) as well as by the low surface area to mass ratio. Even in the shrew, one of the smallest mammals with a large body surface area to mass ratio, the skin contributes not more than 3% of total gaseous metabolism (Mover-Lev et al. 1998). In the neonate quokka wallaby, the epidermis was poorly developed with large amorphous cells, a thin layer of keratin and no hair follicles, making it a weak barrier to transcutaneous traffic and potentially a suitable gas exchange barrier. In the newborn tammar wallaby, which has a similar gestation and birth weight to the quokka, the rate of oxygen consumption through the skin, measured through physiological approaches, was approximately 33% of the total at neonatal day 1 and approximately 14% at day 6 (MacFarlane et al. 2002). The finding of significant exchange across the skin in newborn tammar wallabies, together with the considerable exchange reported in newborns of another marsupial species (*Sminthopsis douglasi*; Mortola et al. 1999), supports the notion that cutaneous exchange in newborn marsupials is commonplace (see MacFarlane et al. 2002). Stucker et al. (2002) have shown that cutaneous diffusion of oxygen for the supply of underlying tissue can reach depths of 250–400 μm, which implies that the epidermal thickness of 30 μm in the neonate quokka is probably not a major hindrance to local gaseous exchange. Percutaneous gas exchange is advantageous in that the animal is exposed to an infinite pool of air with reasonably high partial pressures of oxygen. However, the risk of excessive water loss is high and animals undertaking percutaneous gas exchange need to live in a moist environment. The humid conditions of the pouch in marsupials probably help the joeys circumvent this problem.

Percutaneous traffic of materials depends on the concentration gradient and the diffusion barrier, which is mainly conferred by the stratum corneum. Studies with premature human babies have shown that percutaneous gas exchange rates in the first few days of life were 6–11 times faster in infants below 30 weeks' gestation than in term infants (Cartlidge & Rutter, 1987) and such exchange increased with increasing ambient oxygen concentrations. Gas exchange correlated well with skin water loss, suggesting that the epidermal barrier limits both processes. Skin barrier properties can be explained by the poor development of the stratum corneum in the more premature infants at birth and its rapid maturation after birth (Harpin & Rutter, 1983).

Previous studies have shown the inadequacy of the neonatal marsupial lung (Krause & Leeson, 1973, 1975; Baudinette et al. 1988; Runciman et al. 1996). The newborn opossum (*Didelphis virginiana*) (Frappell & Mortola, 2000) and the tammar wallaby (Runciman et al. 1998b) are characterized by a large resting lung volume. In addition, the presence of surfactant material at birth in the opossum (Krause et al. 1976), quokka wallaby (this study), the tammar wallaby (Ribbons et al. 1989; Miller et al. 2001) and its most likely presence, based on a comparable compliance of the respiratory system, in dunnarts (Frappell & Mortola, 2000) suggests that from the viewpoint of passive mechanics there are no constraints to inspiration. Indeed, surfactant is formed well before birth (Miller et al. 2001; see also reviews by Shaw & Renfree, 2005; Frappell & Macfarlane, 2006). Presumably, dynamic factors related to incompletely developed structures such as respiratory muscles (MacFarlane & Frappell, 2001) and chest-wall distortion (MacFarlane et al. 2002) would also impose constraints to ventilation (MacFarlane & Frappell, 2001). Despite the presence of these several characteristics requisite for gas exchange, the architecture of the lung in the neonate quokkas is critical to sufficient gas exchange. Our findings support the observation that exchange through the skin in newborn marsupials may be a requisite compensation for incomplete pulmonary architecture and dynamic factors that may impede ventilation.

Acknowledgements

We acknowledge financial support from the Swiss National Science Foundation through grant nos. 31-45831.95 and 31-55895.98. We are grateful to the Department of Zoology, University of Western Australia, for providing the specimens on which this study is based. Mr Amos Tangai and Ms Barbara Krieger offered excellent technical assistance. Professor Malcolm Sparrow from the Department of Physiology, University of Western Australia, Perth, supported and facilitated this study. We thank Professor emeritus Ewald Weibel for useful discussions.

References

Baudinette RV, Ganon BJ, Ryall RG, Frapell PB (1988) Changes in metabolic rates and blood respiratory characteristics during pouch development of a marsupial, *Macropus eugenii*. *Respir Physiol* **72**, 219–228.

Burri PH, Weibel ER (1977) Ultrastructure and morphometry of the developing lung. In *Development of the Lung* (ed. Hudson WA), pp. 215–268. New York: Marcel Dekker.

Burri PH (1999) Lung development and pulmonary angiogenesis. In *Lung Development* (eds Gaultier C, Bourbon JR, Post M), pp. 122–151. Oxford: Oxford University Press.

Burri PH, Dbaly J, Weibel ER (1974) The postnatal growth of the rat lung. I. Morphometry. *Anat Rec* **178**, 711–730.

Burri PH, Haenni B, Tschanz SA, Makanya AN (2003) Morphometry and allometry of the postnatal marsupial lung development, an ultrastructural study. *Respir Physiol Neurobiol* **138**, 309–324.

Cartlidge PH, Rutter N (1987) Percutaneous respiration in the newborn infant. Effect of gestation and altered ambient oxygen concentration. *Biol Neonate* **52**, 301–306.

Crapo JD, Young SL, Fram EK, Pinkerton KE, Barry BE, Crapo RO (1983) Morphometric characteristics of the cells in the alveolar region of mammalian lungs. *Am Rev Respir Dis* **128**, 542–546.

Frappell PB, Mortola JP (2000) Respiratory function in a newborn marsupial with skin gas exchange. *Respir Physiol* **120**, 5–45.

Frappell PB, MacFarlane PM (2006) Development of the respiratory system in marsupials. *Respir Physiol Neurobiol* **154**, 252–267.

Gemmell RT, Little GJ (1982) The structure of the lung of the newborn marsupial bandicoot, *Isoodon macrourus*. *Cell Tissue Res* **223**, 445–453.

Hall SM, Hislop AA, Haworth SG (2002) Origin, differentiation and maturation of human pulmonary veins. *Am J Respir Cell Mol Biol* **26**, 333–340.

Harpin VA, Rutter N (1983) Barrier properties of the newborn infant's skin. *J Pediatr* **102**, 419–425.

Humbert D, Cruz-Orive LM, Weibel ER, Gehr P, Burri PH, Hoppeler H (1990) STEPone, an interactive program for manual stereology. *Acta Stereol* **9**, 11–124.

Kauffman SL, Burri PH, Weibel ER (1974) The postnatal growth of the rat lung. II. Autoradiography. *Anat Rec* **180**, 63–76.

Krause WJ, Leeson CR (1973) Postnatal development of the respiratory system of the opossum I, light and scanning microscopy. *Am J Anat* **137**, 337–356.

Krause WJ, Leeson CR (1975) Postnatal development of the respiratory system of the opossum II, Electron microscopy of the epithelium and pleura. *Acta Anat* **92**, 28–44.

Krause WJ, Cutts JH, Leeson CR (1976) Type II pulmonary epithelial cells of the newborn opossum lung. *Am J Anat* **146**, 181–187.

MacFarlane PM, Frappell PB (2001) Convection requirement is established by total metabolic rate in the newborn tammar wallaby. *Respir Physiol* **126**, 221–231.

MacFarlane PM, Frappell PB, Mortola JP (2002) Mechanics of the respiratory system in the newborn tammar wallaby. *J Exp Biol* **205**, 533–538.

Makanya AN, Sparrow MP, Warui CN, Mwangi DK, Burri PH (2001) Morphological analysis of the postnatally developing marsupial lung, the quokka wallaby. *Anat Rec* **262**, 253–265.

Makanya AN, Haenni B, Burri PH (2003) Morphometry and allometry of the postnatal lung development in the quokka wallaby (*Setonix brachyurus*), a light microscopic study. *Respir Physiol Neurobiol* **134**, 43–55.

Makanya AN, Hlushchuk R, Duncker HR, Draeger A, Djonov V (2006) Epithelial transformations in the establishment of the blood–gas barrier in the developing chick embryo lung. *Dev Dyn* **235**, 68–81.

deMello DE, Reid LM (2000) Embryonic and early fetal development of human lung vasculature and its functional implications. *Pediatr Dev Pathol* **3**, 439–449.

Mercurio AR, Rhodin JAG (1976) An electron microscopic study on the type I pneumocyte in the cat, differentiation. *Am J Anat* **146**, 255–272.

Mercurio AR, Rhodin JA (1978) An electron microscopic study on the type I pneumocyte in the cat, pre-natal morphogenesis. *J Morph* **156**, 141–155.

Miller NJ, Orgeig S, Daniels CB, Baudinette RV (2001) Postnatal development and control of the pulmonary surfactant system in the tammar wallaby *Macropus eugenii*. *J Exp Biol* **204**, 4031–4042.

Mortola J, Frapell PB, Woolley PA (1999) Breathing through skin in a newborn mammal. *Nature* **397**, 660.

Mover-Lev H, Minzberg H, Ar A (1998) Is there a significant gas exchange through the skin of the shrew, *Crocidura russula monacha*? *Physiol Zool* **71**, 407–413.

Ribbons KA, Baudinette RV, McMurchie EJ (1989) The development of the pulmonary surfactant lipids in a neonatal marsupial and the rat. *Respir Physiol* **75**, 1–10.

Runciman SIC, Baudinette RV, Cannon B (1996) Postnatal development of the lung parenchyma in a marsupial, the tammar wallaby. *Anat Rec* **244**, 193–206.

Runciman SI, Baudinette RV, Gannon BJ, Lipsett J (1998) Morphometric estimate of gas-exchange tissue in the new-born tammar wallaby, *Macropus eugenii*. *Respir Physiol* **111**, 177–187.

Runciman SI, Baudinette RV, Gannon BJ, Lipsett J (1999) Morphometric analysis of postnatal lung development in a marsupial, transmission electron microscopy. *Respir Physiol* **118**, 61–75.

Scherle WF (1970) A simple method for volume try of organs in quantitative stereology. *Mikroskopie* **26**, 57–60.

Schittny JC, Djonov V, Fine A, Burri PH (1998) Programmed cell death contributes to postnatal lung development. *Am J Respir Cell Mol Biol* **18**, 786–793.

Schittny JC, Burri PH (2003) Morphogenesis of the mammalian lung, aspects of structure and extracellular matrix components. In *Lung Development and Regeneration* (eds Massaro DJ, Massaro G, Chambon P), pp. 275–317. New York: Dekker .

Shaw G, Renfree MB (2005) Parturition and perfect prematurity, birth in marsupials. *Aust J Zool* **54**, 139–149.

Spearman RIC (1968) Epidermal keratinization in the salamander and a comparison with other amphibia. *J Morph* **125**, 129–143.

Stiles AD, Chrysis D, Jarvis HW, Brighton B, Moats-Staats BM (2001) Programmed cell death in normal fetal rat lung development. *Exp Lung Res* **27**, 569–587.

Stucker M, Struk A, Altmeyer P, Herde M, Baumgartl H, Lubbers DW (2002) The cutaneous uptake of atmospheric oxygen contributes significantly to the oxygen supply of human dermis and epidermis. *J Physiol* **538**, 985–994.

Weibel ER (1979) *Stereological Methods, Practical Methods for Biological Morphometry*, Vol. I. London: Academic Press.

Weibel ER, Federspiel WJ, Fryder-Doffey F, et al. (1993) Morphometric model for pulmonary diffusing capacity. I. Membrane diffusing capacity. *Respir Physiol* **93**, 125–149.

Whitford WG, Hutchison VH (1965) Gas exchange in salamanders. *Physiol Zool* **38**, 228–242.